0.1 3 Residual Contributors Included in Fit

This section presents our final results, for which three residual contributors were assumed. These three contributors include: (Σ^0K, Ξ^0K, Ξ^-K) $\rightarrow$ ΛK. The figures presented do contain supplemental information to that presented in Sec. **??**, but are here largely for convenience in comparing to the cases of including 10 (App. **??**) and no (App. **??**) residual contributors.

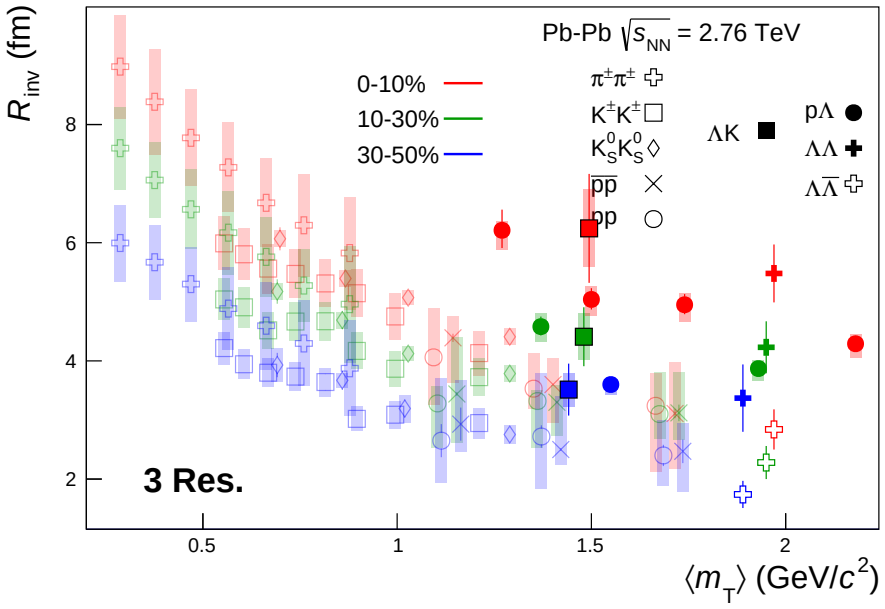

Figure 0.1: 3 residual correlations in ΛK fits. Extracted fit $R_{\rm inv}$ parameters as a function of pair transverse mass ($m_{\rm T}$) for various pair systems over several centralities. The ALICE published data [**?**] are shown with transparent, open symbols. The new ΛK results are shown with opaque, filled symbols. The $m_{\rm T}$ value for the ΛK system is an average of those for the ΛK^+, $\bar{\Lambda} K^-$, and ΛK^0_S systems.

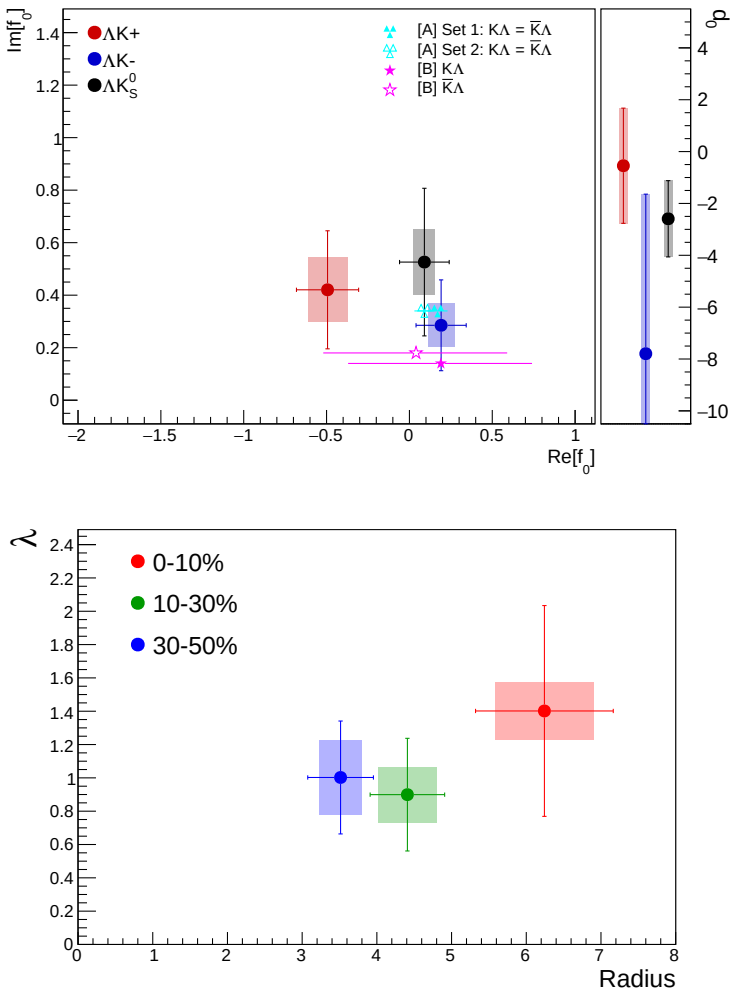

Figure 0.2: Extracted fit parameters for the case of 3 residual contributors for all of our ΛK systems. [Top]: $\Im f_0$ vs. $\Re f_0$, together with d_0 to the right. [Bottom]: λ vs. Radius for the 0-10% (blue), 10-30% (green), and 30-50% (red) centrality bins. In the fit, all ΛK systems share common radii. The color scheme used in the panel are to be consistent with those in Fig. 0.1. The cyan ([A] = Ref. [**?**]) and magenta ([B] = Ref. [**?**]) points show theoretical predictions made using chiral perturbation theory.

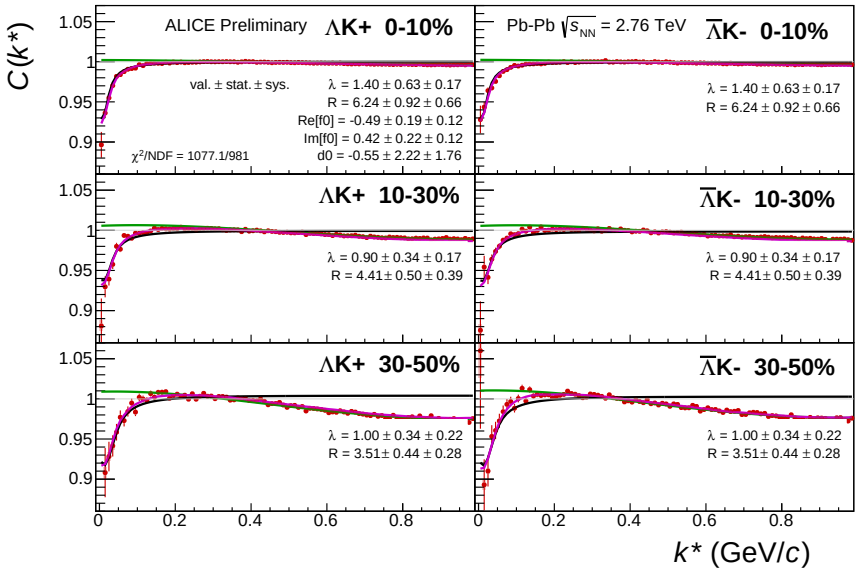

Figure 0.3: Fit results, with 3 residual correlations included, for the ΛK^+ and $\bar{\Lambda} K^-$ data. The ΛK^+ data is shown in the left column, the $\bar{\Lambda} K^-$ in the right, and the rows differentiate the different centrality bins (0-10% in the top, 10-30% in the middle, and 30-50% in the bottom).

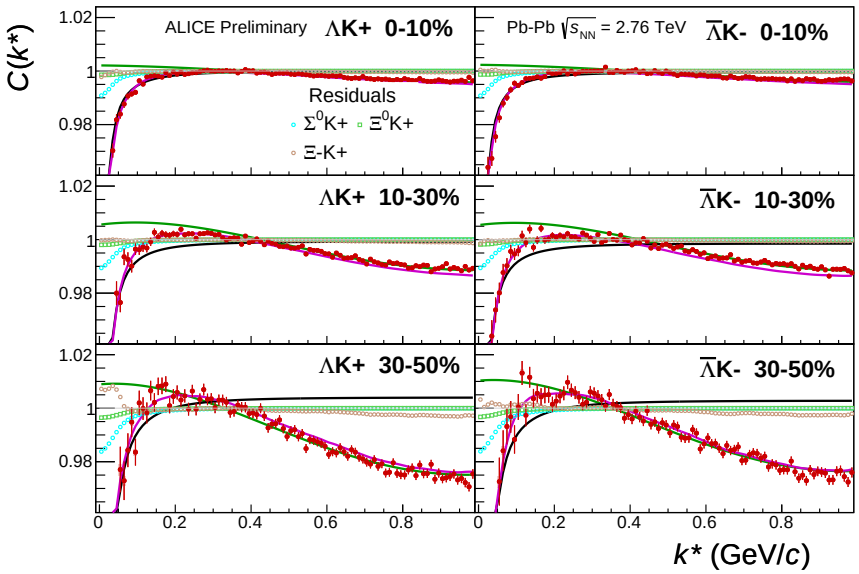

Figure 0.4: Fit results with the 3 residual contributions shown, for the ΛK^+ and $\bar{\Lambda} K^-$ data. The ΛK^+ data is shown in the left column, the $\bar{\Lambda} K^-$ in the right, and the rows differentiate the different centrality bins (0-10% in the top, 10-30% in the middle, and 30-50% in the bottom).

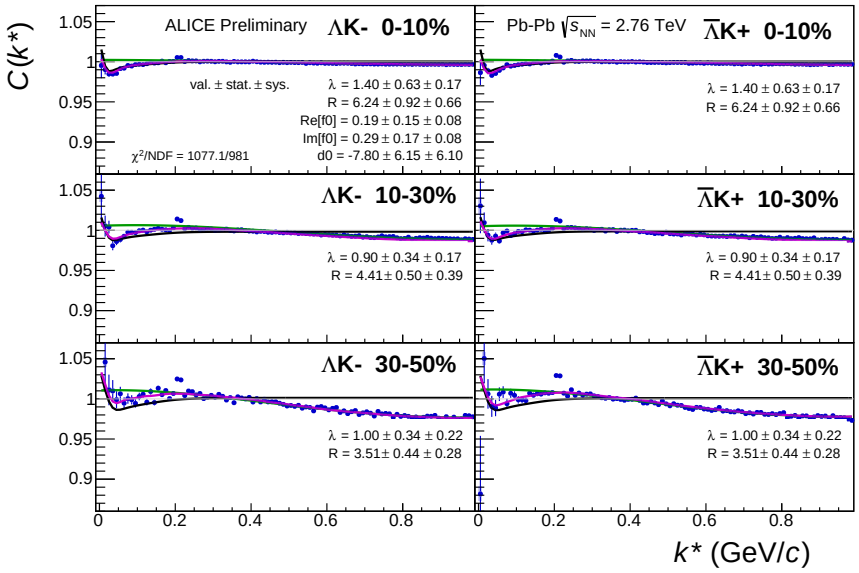

Figure 0.5: Fit results, with 3 residual correlations included, for the ΛK^- and $\bar{\Lambda}K^+$ data. The ΛK^- data is shown in the left column, the $\bar{\Lambda}K^+$ in the right, and the rows differentiate the different centrality bins (0-10% in the top, 10-30% in the middle, and 30-50% in the bottom).

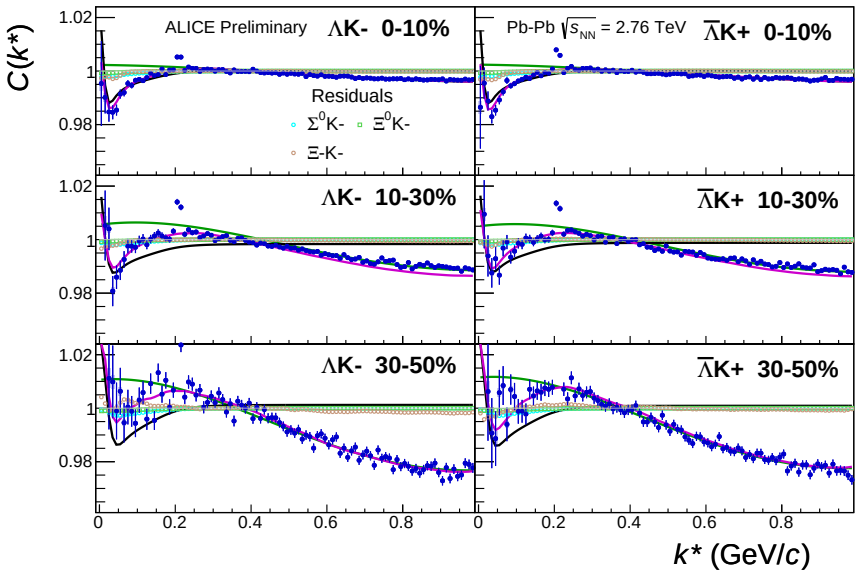

Figure 0.6: Fit results with the 3 residual contributions shown, for the ΛK^- and $\bar{\Lambda}K^+$ data. The ΛK^- data is shown in the left column, the $\bar{\Lambda}K^+$ in the right, and the rows differentiate the different centrality bins (0-10% in the top, 10-30% in the middle, and 30-50% in the bottom).

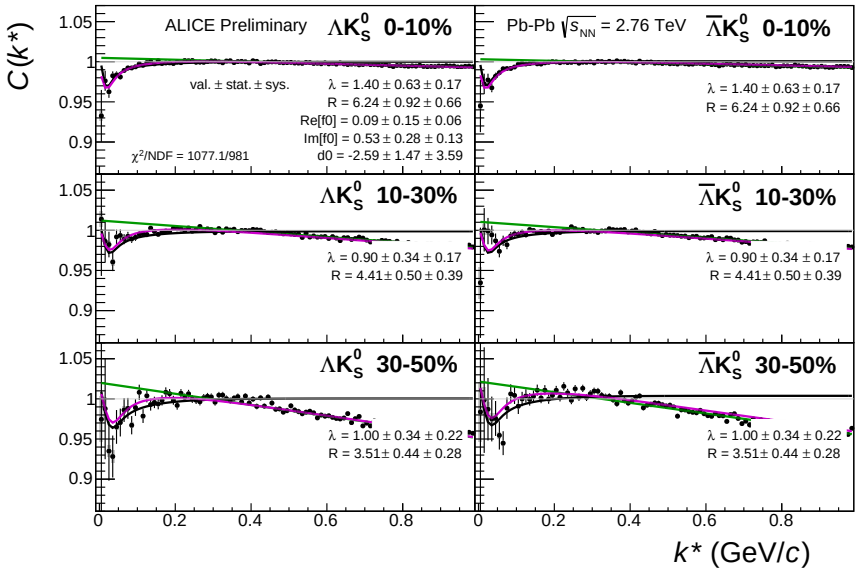

Figure 0.7: Fit results, with 3 residual correlations included, for the ΛK^0_S and $\bar{\Lambda}K^0_S$ data. The ΛK^0_S data is shown in the left column, the $\bar{\Lambda}K^0_S$ in the right, and the rows differentiate the different centrality bins (0-10% in the top, 10-30% in the middle, and 30-50% in the bottom).

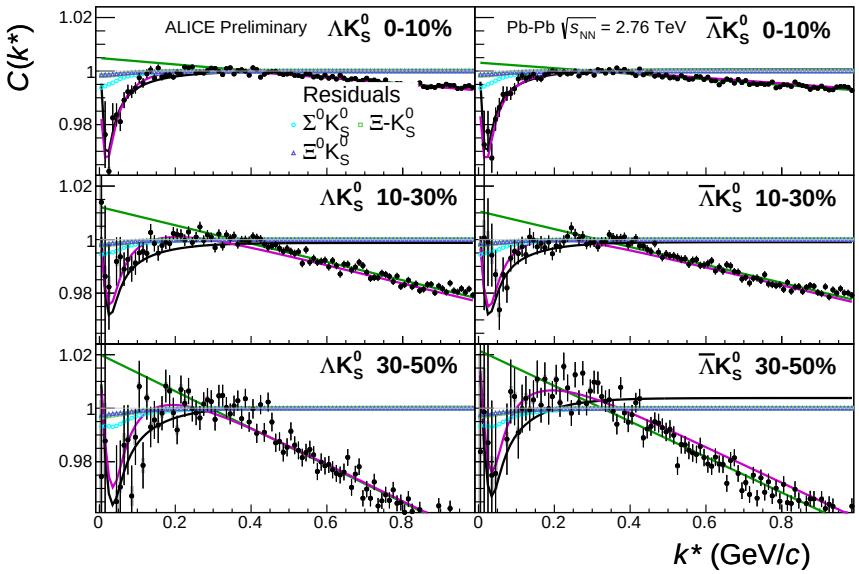

Figure 0.8: Fit results with the 3 residual contributions shown, for the ΛK^0_S and $\bar{\Lambda}K^0_S$ data. The ΛK^0_S data is shown in the left column, the $\bar{\Lambda}K^0_S$ in the right, and the rows differentiate the different centrality bins (0-10% in the top, 10-30% in the middle, and 30-50% in the bottom).